The Joubert Syndrome Protein Inpp5e Controls Ciliogenesis by Regulating Phosphoinositides at the Apical Membrane in Zebrafish

Wenyan Xu[1], Miaomiao Jin[1], Ruikun Hu[1], Hong Wang[1], Fan Zhang[1], Shiaulou Yuan[2] and Ying Cao[1,3]*

1. Department of Molecular and Cell Biology, Tongji University School of Life Sciences and Technology, 1239 Siping Road, Medical Building 1315, Shanghai 200092, P. R. China

2. Department of Pediatrics, Yale University School of Medicine, 15 York St, FMP 424, New Haven, CT 06510, USA

3. Tongji University and Shanghai Changzheng Hospital Joint Research Center for Translational Medicine, 800 Xiangyin Road, Shanghai 200092, P. R. China

*author for correspondence (email: **yingcao@tongji.edu.cn**; phone: 086-21-6598-6033; fax: 086-21-6598-6033)

Running Title:

Phosphoinositides and Cilia

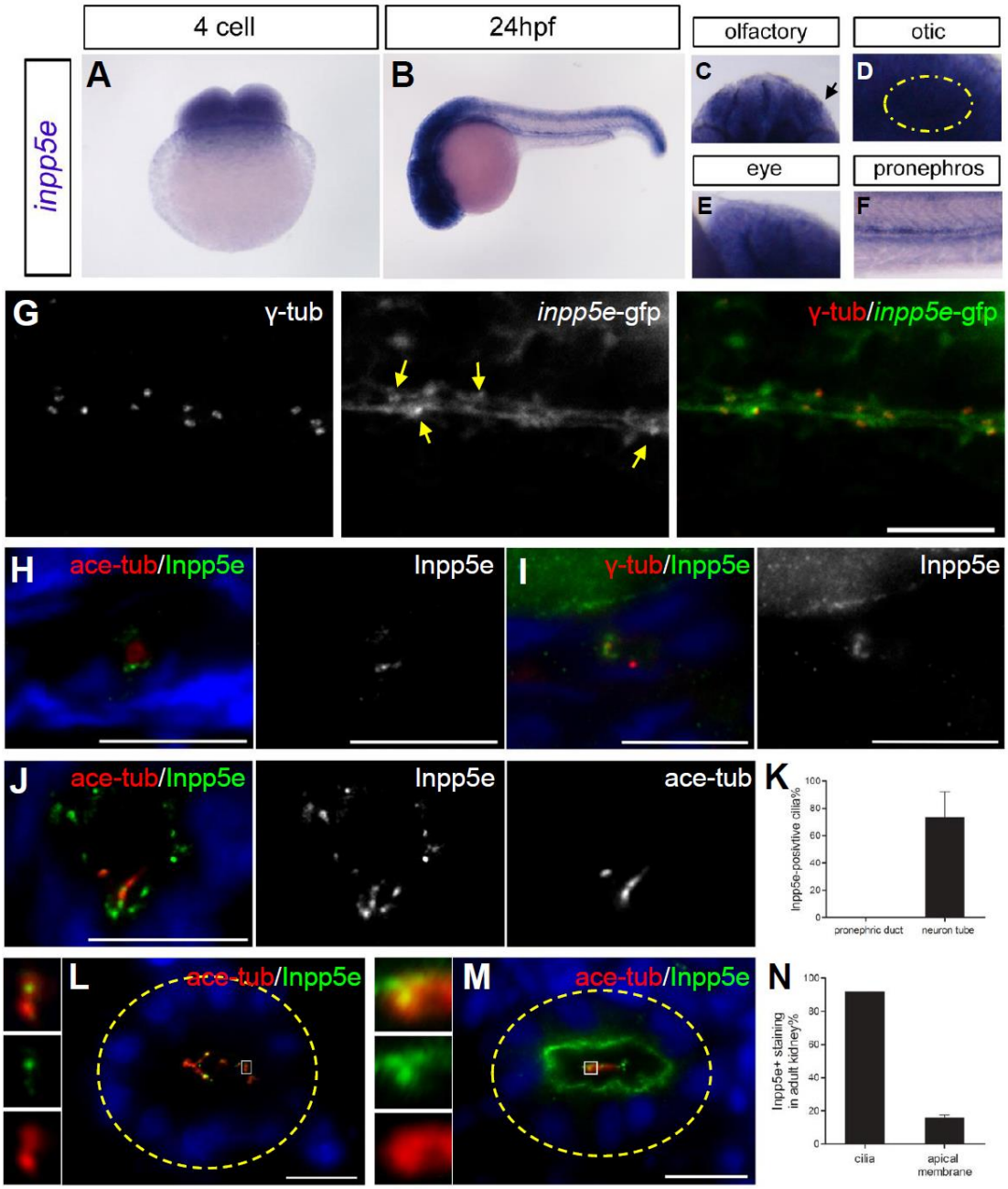

Supplemental Figure 1: Expression pattern and subcellular localization of transcript and encoding protein of *inpp5e*. Dorsal view in figure C, E and side view in figure A, B, D, F, G. (A-F) Expression pattern of *inpp5e* transcript in zebrafish embryos at 4-cell stage (A) and 24 hpf (B-F). Black arrow points the expression of *inpp5e* transcript in olfactory vesicle and yellow dotted circle indicates the otic vesicle. (G) Fluorescent image of the pnd in *inpp5e-gfp* overexpressed embryos stained with antibody against basal body marker γ-Tub. Yellow arrows indicate localization of Inpp5e-GFP in basal bodies. (H, I) Cross sections of the pnd from embryos stained with

antibodies against Inpp5e and ace-Tub (H) or γ-Tub (I). (J) Cross sections of the neural tube stained with antibodies against Inpp5e and ace-Tub. (K) Bar graph shows the percentage of ciliary staining of Inpp5e in pnd or neural tubes. N=2, n≥100 cilia from 9 embryos. (L, M) Cross sections of the adult zebrafish kidney stained with antibodies against Inpp5e and ace-Tub. Insets on the left show magnification of the ciliary staining of Inpp5e in the white-boxed region in the main figure. Yellow dotted circles indicate the kidney tubule region. (N) Bar graph shows the percentage of ciliary or apical staining of Inpp5e in adult kidneys. N=2, n≥100 sections from 4 kidneys. Scale bar: 10 μm.

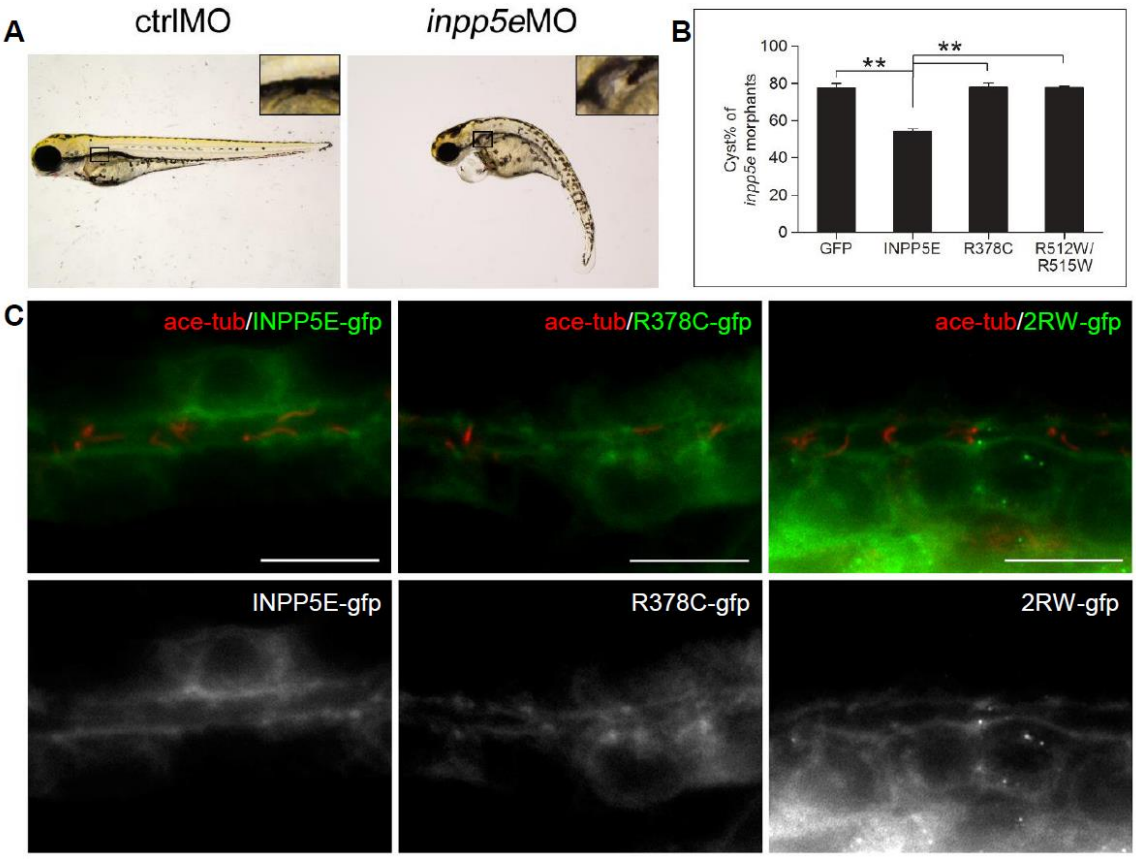

Supplemental Figure 2: *inpp5e* morphants can be rescued by overexpression of INPP5E-GFP, but not catalytically dead form of INPP5E, INPP5E-R378C-GFP or INPP5E-R512/515W-GFP. Side view in all figures (A) Representative images of ctrl morphant and *inpp5e* morphant at 72 hpf. Insets show magnification of glomerulus area in black-boxed region in main figure. (B) Bar graph shows that percentage of cystic kidney is significantly reduced in *inpp5e* morphants with INPP5E-GFP, but not INPP5E-R378C-GFP or INPP5E-R512/515W-GFP. Error bars, s.d. **, 0.005<p<0.01. (C) Fluorescent images of the pnd from embryos injected with *INPP5E-GFP* or *INPP5E-R378C-GFP* or *INPP5E-R512/515W-GFP* mRNA and stained with antibodies against GFP and ace-Tub. Scale bar: 10 μm.

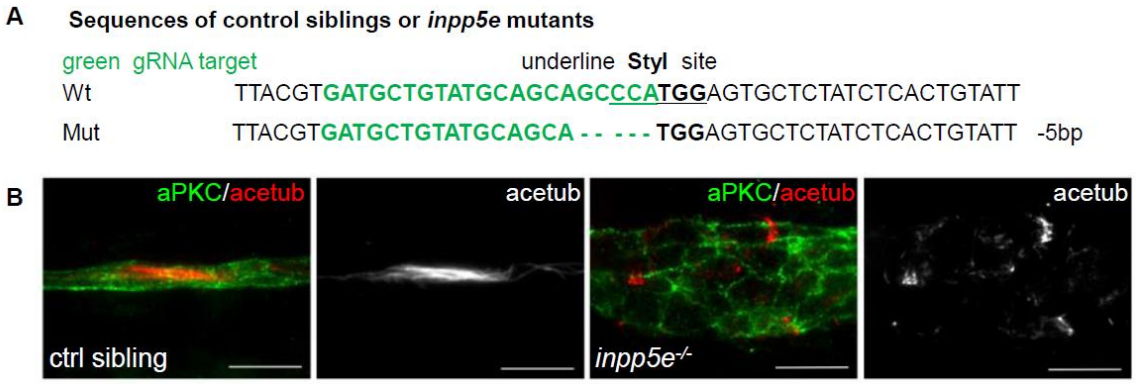

Supplemental Figure 3: Characterization of *inpp5e* mutant. (A) DNA sequences of gRNA target site from *inpp5e* mutants compared to that from wild type. (B) Representative fluorescent images of multi-ciliated cells from the pnd of *ctrl* siblings or *inpp5e* mutants at 3 dpf stained with antibodies against aPKC and ace-Tub. Scale bar: 20 μm.

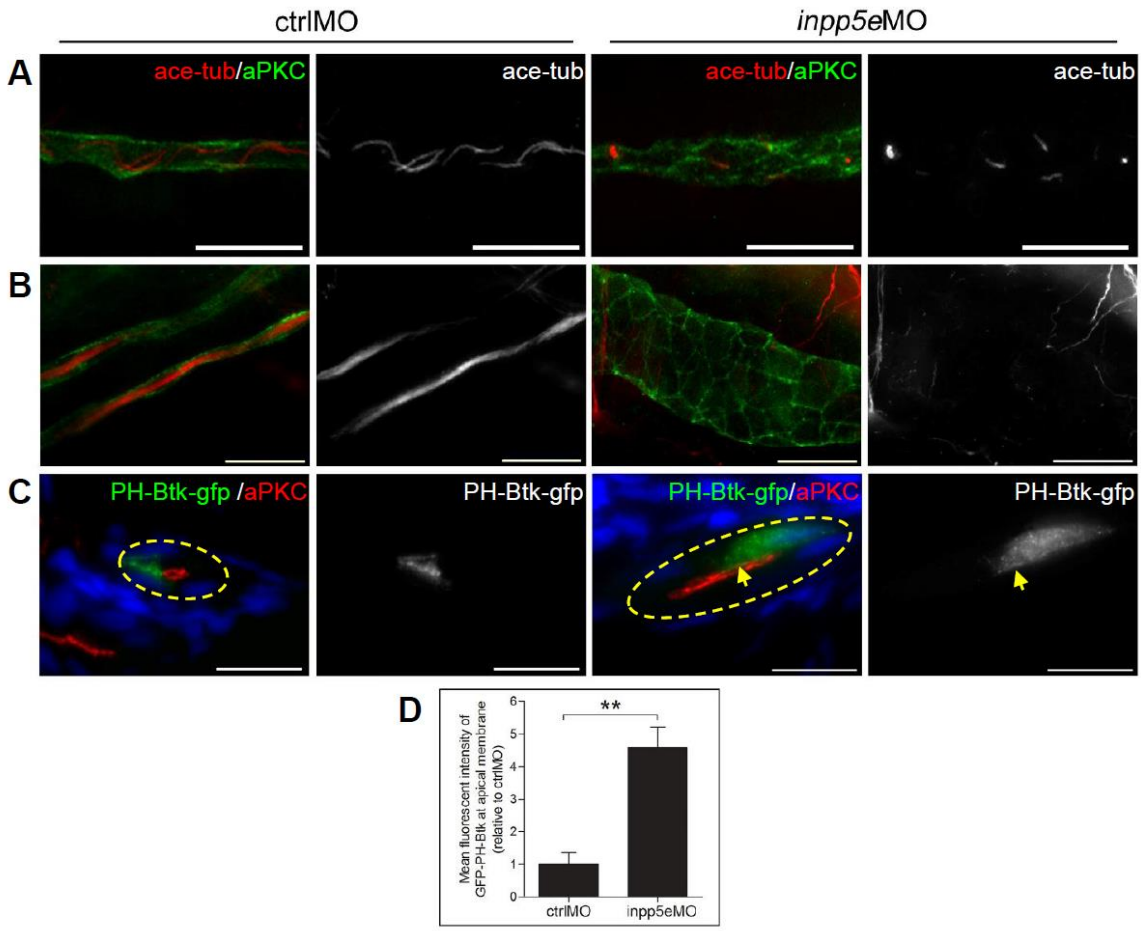

Supplemental Figure 4: Cellular defects in the pronephric epithelium of *inpp5e* morphants. (A, B) Representative images of the single-ciliated cells (B) or multi-ciliated cells (C) of the pnd in *ctrl* morphants or *inpp5e* morphants stained with antibodies against acetylated Tub (red, cilia) and aPKC (green, apical of pnd). (C) Fluorescent images of cross sections of *ctrl* morphants (left) or *inpp5e* morphants (right) injected with Cdh17-PH-Btk-gfp plasmid and followed by immunostaining with antibodies against GFP and a-PKC. Yellow dotted circles indicate the pnd area. Yellow arrow indicates the apical mislocalization of PtdIns(3,4,5)P3. (D) Scale bar of the apical localization of PtdIns(3,4,5)P3 indicated by fluorescent intensity of PH-Btk-GFP. Error bar: s.d. **: 0.005<p<0.01. Scale bar: 10 μm.

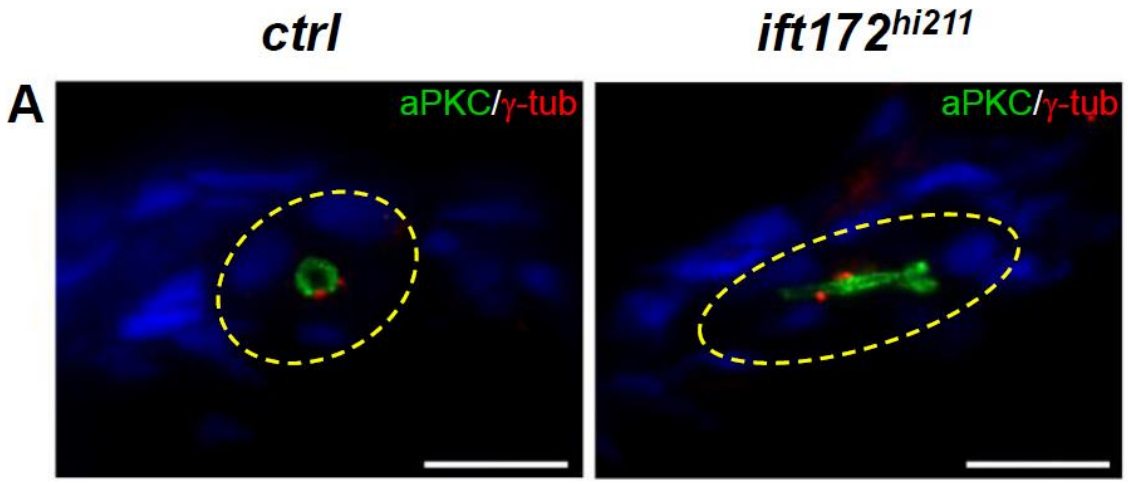

Supplemental Figure 5: Localization of basal bodies in *ift172*^{hi2211} mutants. Embryos are at 3 dpf. Controls are on the left and mutants on the right. Cross sections of *ift172*^{hi2211} mutants (81.3%, n=16 pooled from 2 independent experiments) and of its *ctrl* siblings (100%, n=10 pooled from 2 independent experiments) stained with antibodies against aPKC and γ-Tub. Yellow dotted circles indicate the pnd area. Scale bar: 10 μm.

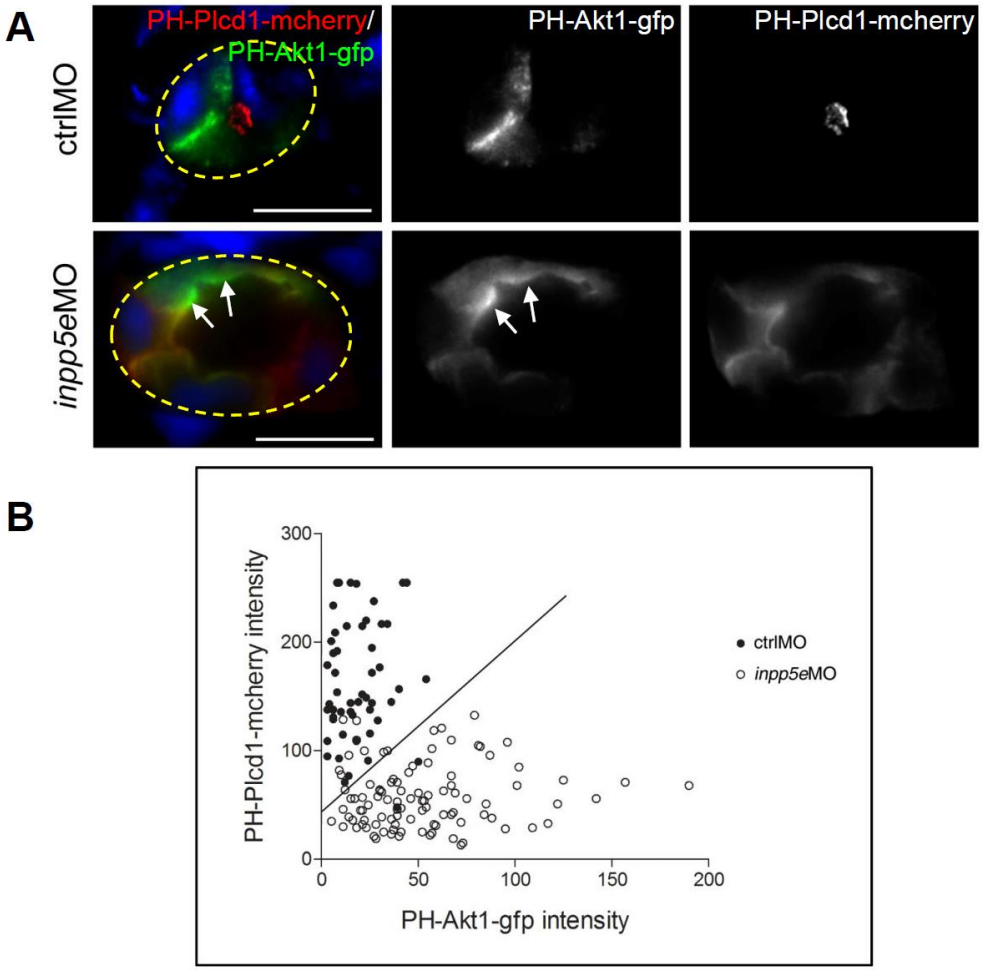

Supplemental Figure 6: Apical segregation of PtdIns(4,5)P_2 and PtdIns(3,4,5)P_3 are disrupted in *inpp5e* morphants. (A) Cross sections of pnd area from *Tg(Tolcdh17:akt1-gfp;Tolcdh17:plcd1-mcherry)* double transgenic embryos injected with control morpholino (top) or *inpp5e* morpholino (bottom). Yellow-dotted circles indicate the pnd and white arrows indicate the apical localization of PtdIns(3,4,5)P_3. Scale bar: 10 μm. (B) Scatter Plot shows the apical fluorescence intensity of PH-Plcd1-mcherry versus that of PH-Akt1-GFP. Black dots represent control morphants and white represent *inpp5e* morphants. Note that the distribution of black dots and white dots are segregated in the plot with 96.1% of the black dots (n=52) above the line while 92% of the white dots (n=100) under the line, indicating that majority of the control morphants have high intensity of PH-Plcd1-mcherry while low intensity of PH-Akt1-GFP at the apical membrane, which is opposite in *inpp5e* morphants.

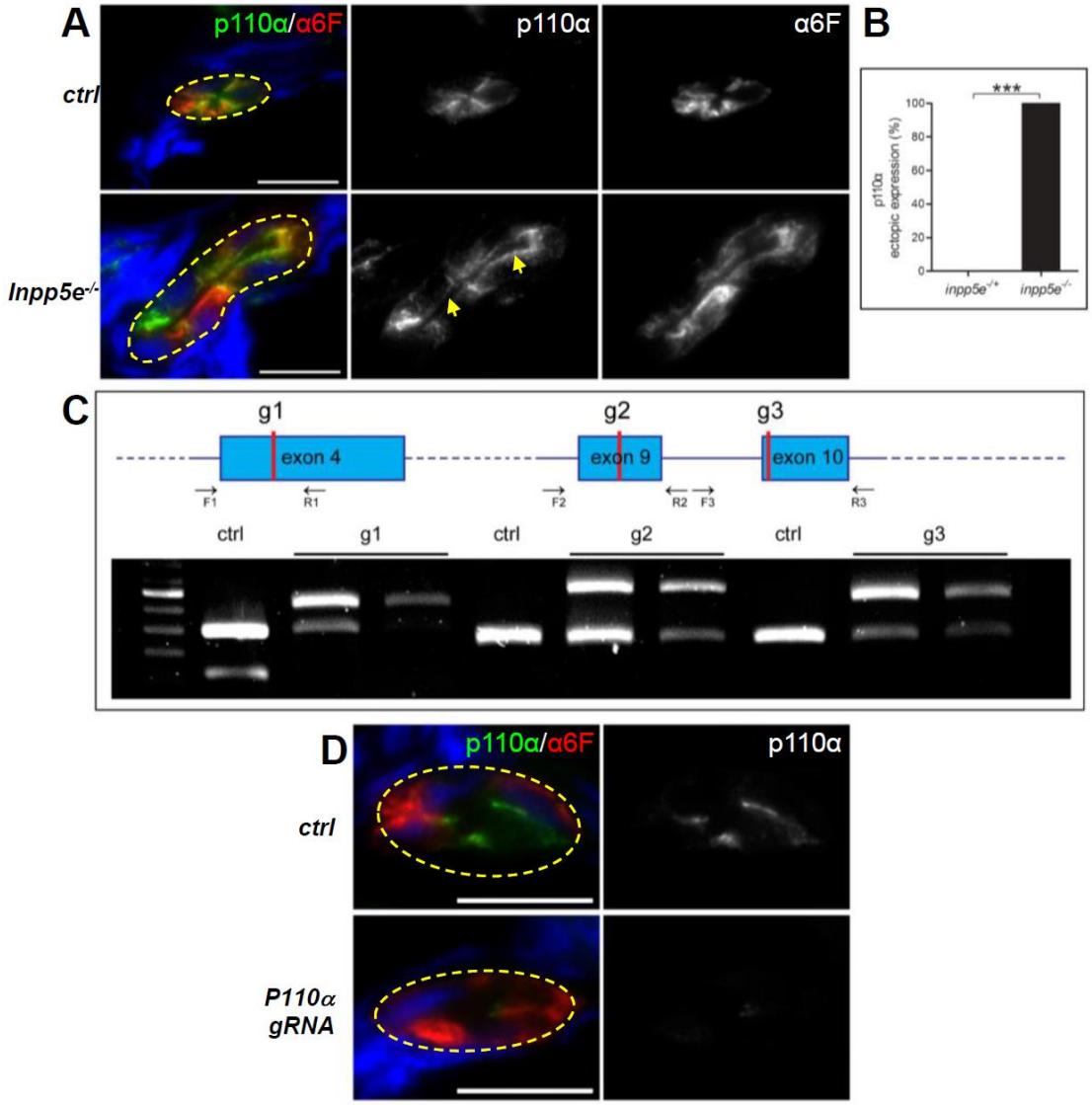

Supplemental Figure 7: Subcellular localization of p110a in *inpp5e* mutants. Figure A, D, cross sections of pnd area of the embryos. Figure A, C, control on the top and mutant on the bottom. (A) Fluorescent images of cross sections from *ctrl* siblings and *inpp5e*$^{-/-}$ mutants stained with antibodies against p110α and basolateral marker a6F. Yellow arrows indicate the apical mislocalization of p110α. (B) Bar graph of percentage of apically mislocalized p110α in *ctrl* siblings and *inpp5e*$^{-/-}$ mutants. N=2, n≥8. ***: p≤0.005. (C) Schematic image of genomic localization of three gRNAs targeting *p110α* (top) and gel electrophoresis analysis of PCR amplified fragment from genomic lysate of *ctrl* embryos or three *p110α*-gRNAs injected embryos followed by restriction enzyme digestion (bottom). For each gRNA, the mutagenesis efficiency is around 50%-70%, estimated from the digestion pattern. (D) Fluorescent images of pnd section of *ctrl* embryos or three *p110α*-gRNAs injected embryos stained with antibodies against p110*α* and *α*6F. Yellow dotted lines circle the pnd area. Scale bar: 10 μm.

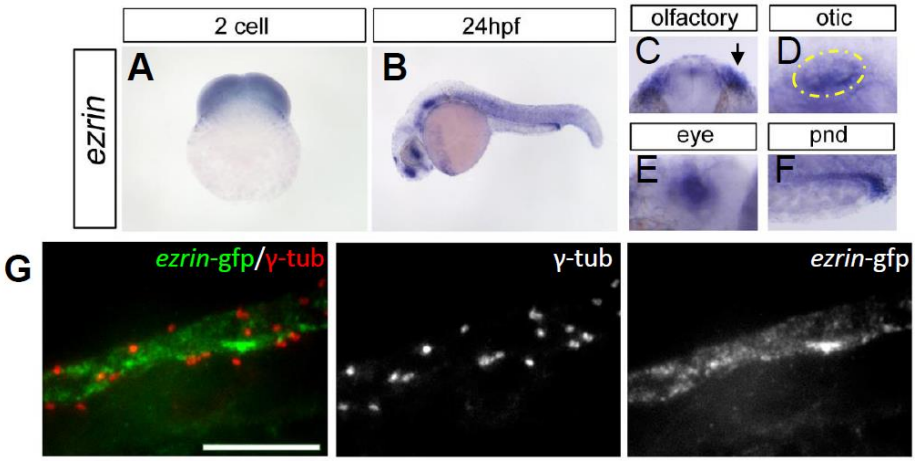

Supplemental Figure 8: Expression and subcellular localization of *ezrin* transcript and protein. (A-F) Expression of *ezrin* at 2-cell stage (A) and at 24 hpf (B-F). Dorsal view for C and E, lateral view for the rest. Arrow points to olfactory vesicle (C) and yellow dotted circle indicates otic vesicle (D). (G) Apical localization of Ezrin indicated by embryos injected with *ezrin-gfp* and stained with antibody against γ-Tub. Scale bar: 10 μm.

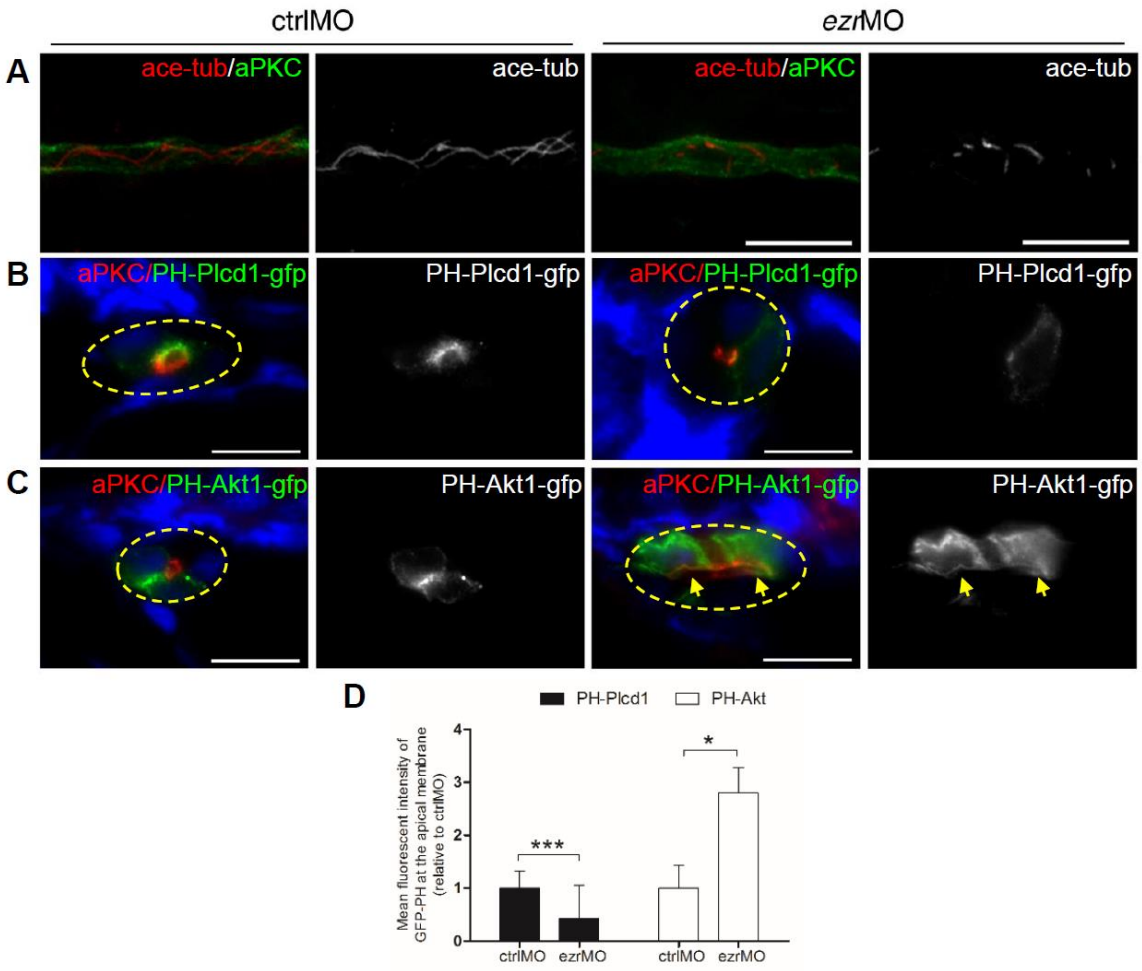

Supplemental Figure 9: Cellular defects in the pnd of *ezrin* morphants. (A) Fluorescent image of pnd from embryos injected with *ctrl* MO (left) or *ezrin* MO (right) and stained with antibodies against aPKC (green) and ace-Tub (red). Note ciliary defect in single-ciliated cells of *ezrin* morphants. (B) Fluorescent image of pnd sections from transgenic *Tg(cdh17:PH-Plcd1-gfp)* (B) or *Tg(cdh17:PH-Akt1-gfp)* lines injected with *ctrl* MO (left) or *ezrin* MO (right) and stained with antibodies against GFP and a-PKC. Yellow dotted lines circle the pnd area and yellow arrows indicate apically mislocalized PtdIns(3,4,5)P3/PH-Akt1-GFP. (D) Bar graph of fluorescent intensity of apically localized PtdIns(4,5)P2/PH-Plcd1-GFP and PtdIns(3,4,5)P3/PH-Akt1-GFP in *ezrin* morphants compared to *ctrl* morphants. Fluorescent intensity is normalized to 1 in *ctrl* morphants. N=2, n≥40 cells from 7~8 embryos. Error bar: s.d. *: 0.01≤p≤0.05. ***: p≤0.005. Scale bar: 10 μm.

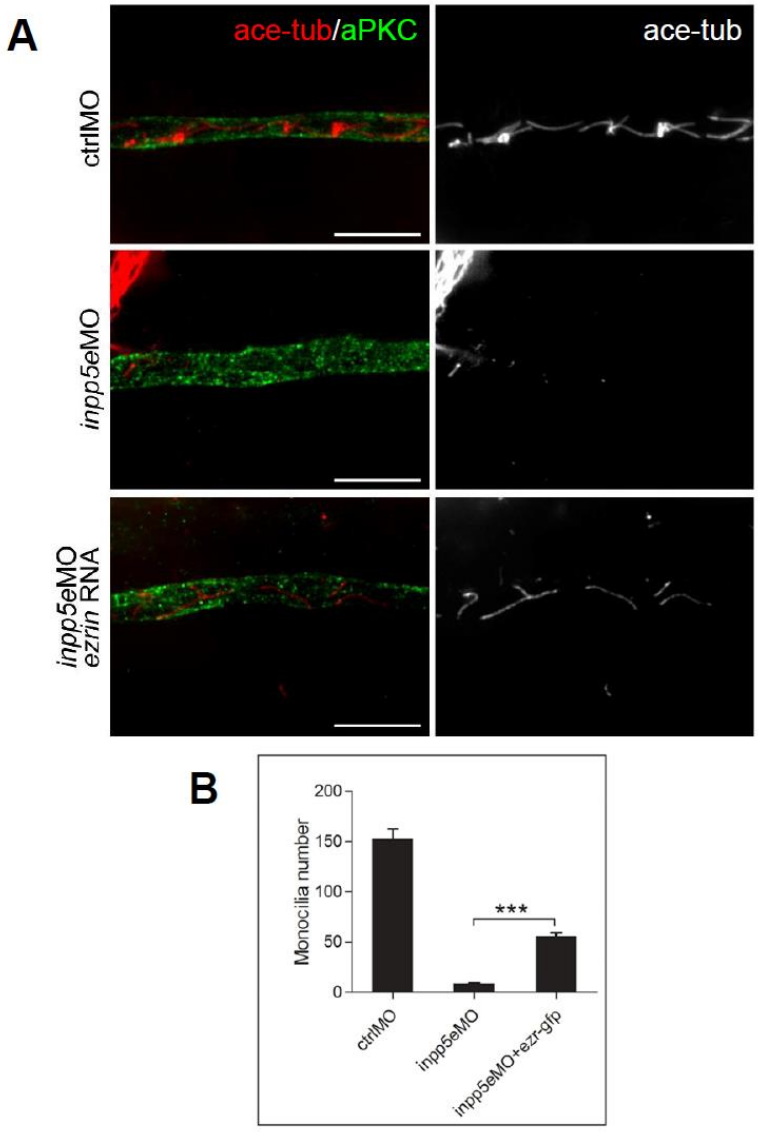

Supplemental Figure 10: *ezrin* mRNA overexpression restores ciliogenesis in *inpp5e* morphants. (A) Fluorescent images of embryos injected with *ctrl* morpholino (top row), or *inpp5e* morpholino (middle row), or *inpp5e* morpholino combined with *ezrin* mRNA (bottom row), and stained with antibody against acetylated-Tubulin or aPKC. (B) Bar graph shows that cilia number of single-ciliated cells from distal region of the pnd in the indicated groups (N=2, n≥6). Scale bar: 10 μm. ***, p<0.005.

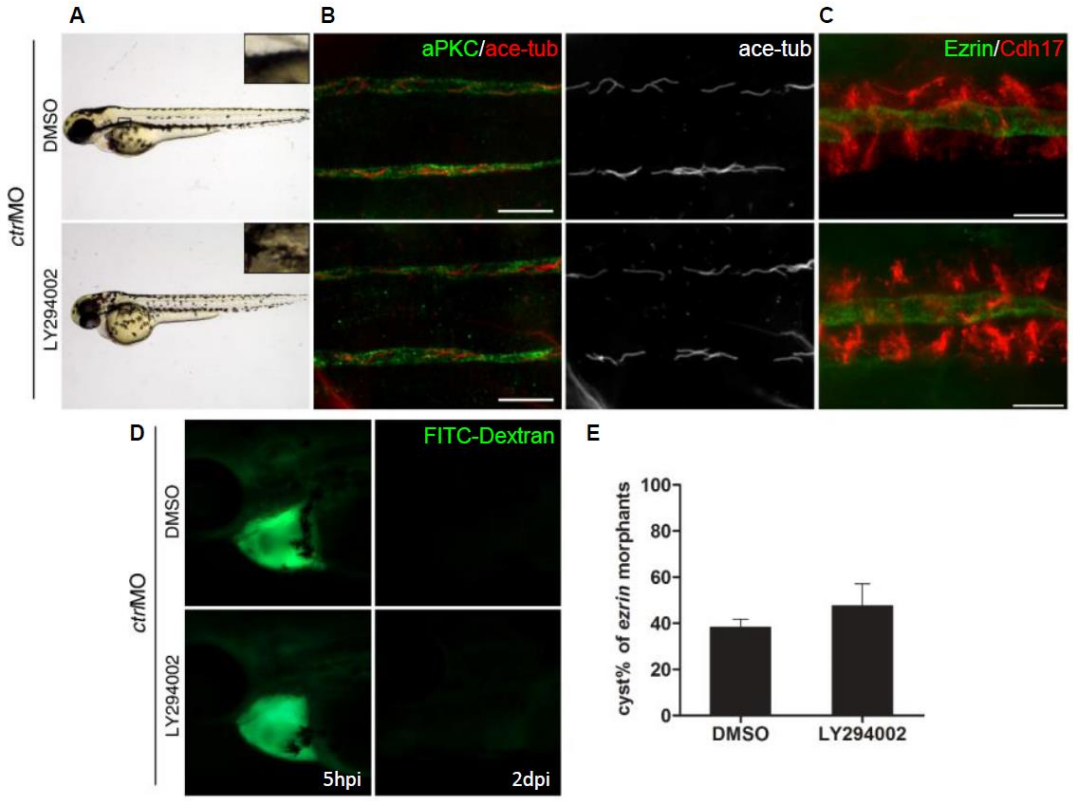

Supplemental Figure 11: 15 μM of LY294002 has little effect on embryonic development. Embryos in all figures are *ctrl* morphants at 3 dpf treated with vehicle (DMSO, top row) or 15 μM of LY294002 (bottom row) from 50% epiboly stage. (A) Representative images of live embryos show overall normal phenotype of embryos treated with 15 μM LY294002. Insets show magnification of the glomerulus area in black-boxed region. (B) Representative images of pnd region in embryos stained with antibodies against aPKC and ace-Tub show normal cilia in LY294002 treated embryos. Scale bar: 20 μm. (C) Representative images of pnd region in embryos stained with antibodies against Ezrin and Cdh17 show normal apical localization of Ezrin in LY294002 treated embryos. Scale bar: 10 μm. (D) Fluorescent images of heart region of embryos after 5 hours (left column) or 2 days (right column) post injection with FITC-Dextran. (E) Bar graph shows cystic kidney in *ezrin* morphants treated with or without LY294002. N=2, n≥21. Error bar: s.d. Scale bar: 10 μm.

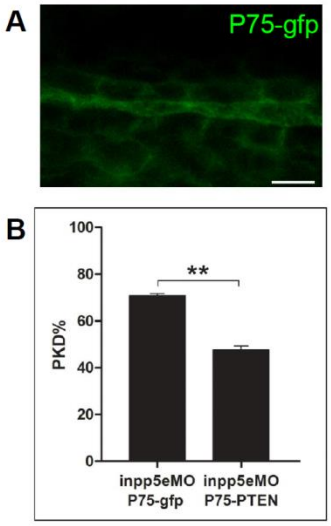

Supplemental Figure 12: Overexpression of p75-PTEN suppresses cystic kidney in *inpp5e* morphants. (A) Fluorescent images of pnd area from p75-GFP overexpressed embryos show that p75-GFP is enriched on the apical membrane. Scale bar: 10 μm. (B) Bar graph of cystic kidney percentage in *inpp5e* morphants coinjected with *p75-gfp* or *p75-PTEN* mRNA. N=2, n>65. **, $0.005<p\leqslant 0.01$.